quantum reports

MDPI

Article

Quantum Computing, Seifert Surfaces, and Singular Fibers

Michel Planat [1,*], Raymond Aschheim [2], Marcelo M. Amaral [2] and Klee Irwin [2]

[1] Institut FEMTO-ST CNRS UMR 6174, Université de Bourgogne/Franche-Comté, 15 B Avenue des Montboucons, F-25044 Besançon, France

[2] Quantum Gravity Research, Los Angeles, CA 90290, USA; raymond@QuantumGravityResearch.org (R.A.); Marcelo@quantumgravityresearch.org (M.M.A.); Klee@quantumgravityresearch.org (K.I.)

* Correspondence: michel.planat@femto-st.fr

Received: 11 March 2019; Accepted: 17 April 2019; Published: 24 April 2019

Abstract: The fundamental group $\pi_1(L)$ of a knot or link L may be used to generate magic states appropriate for performing universal quantum computation and simultaneously for retrieving complete information about the processed quantum states. In this paper, one defines braids whose closure is the L of such a quantum computer model and computes their braid-induced Seifert surfaces and the corresponding Alexander polynomial. In particular, some d-fold coverings of the trefoil knot, with $d = 3$, 4, 6, or 12, define appropriate links L, and the latter two cases connect to the Dynkin diagrams of E_6 and D_4, respectively. In this new context, one finds that this correspondence continues with Kodaira's classification of elliptic singular fibers. The Seifert fibered toroidal manifold Σ', at the boundary of the singular fiber $\tilde{E_8}$, allows possible models of quantum computing.

Keywords: quantum computing; Seifert surfaces; singular fibers

1. Introduction

To acquire computational advantage over a classical circuit, a quantum circuit needs a non-stabilizer quantum operation for preparing a non-Pauli eigenstate, often called a magic state. The work about qubit magic state distillation [1] was generalized to qudits [2] and multi-qubits (see [3] for a review). Thanks to these methods, universal quantum computation (UQC), the ability to prepare every quantum gate, is possible. A new approach of UQC, based on permutation gates and simultaneously minimal informationally-complete positive operator-valued measures (MICs), was worked out in [4,5]. It is notable that the structure of the projective special linear group (or modular group) Γ is sufficient for getting most permutation-based magic states [6] used by us for UQC and that this can be thought of in terms of the complement of the trefoil knot in the three-sphere S^3 [7].

Let us recall the context of our work compared to the existing literature. Bravyi and Kitaev introduced the principle of "magic state distillation" [1]: universal quantum computation, the possibility of getting an arbitrary quantum gate, may be realized thanks to stabilizer operations (Clifford group unitaries, preparations, and measurements) and an appropriate single qubit non-stabilizer state, called a "magic state". Then, irrespective of the dimension of the Hilbert space where the quantum states live, a non-stabilizer pure state was called a magic state [2]. An improvement of this concept was carried out in [4,5] showing that a magic state could be at the same time a fiducial state for the construction of a minimal informationally-complete positive operator-valued measure (MIC) under the action on it of the Pauli group of the corresponding dimension. Thus, UQC in this view happens to be relevant both to magic states and to MICs. In [4,5], a d-dimensional magic state was obtained from the permutation group that organizes the cosets of a subgroup H of index d of a two-generator free group G. This is due to the fact that a permutation

matrix/gate and that mutually-commuting matrices share eigenstates: they are either of the stabilizer type (as elements of the Pauli group) or of the magic type. It is enough to keep magic states that are simultaneously fiducial states for an MIC because the other magic states may loose the information carried during the computation. A catalog of the magic states relevant to UQC and MICs can be obtained by selecting G as the two-letter representation of the modular group $\Gamma = PSL(2,\mathbb{Z})$ [6]. The next step, developed in [7], is to relate the choice of the starting group G to a three-dimensional topology. More precisely, G is taken as the fundamental group $\pi_1(S^3 \setminus L)$ of a three-manifold M^3 defined as the complement of a knot or link L in the three-sphere S^3. A branched covering of degree d over the selected M^3 has a fundamental group corresponding to a subgroup of index d of $\pi_1(M^3)$ and may be identified as a sub-manifold of M^3; the one leading to an MIC is a model of UQC. In the specific case of Γ, the knot involved is the left-handed trefoil knot $T_1 = 3^1$, as shown in [6] and [7] (Section 2).

1.1. Motivation of the Work

It is desirable that the UQC approach of [4–7] be formulated in terms of braid theory to allow a physical implementation. Braids of the anyon type, which are two-dimensional quasiparticles with world lines creating space-time braids, are currently very popular [8–10]. Close to this view of topological quantum computation (TQC) based on anyons, we propose a TQC based on a Seifert surface defined over a link L. The links in question will be those able to generate magic states appropriate for performing permutation-based UQC. In our previous work [7], we investigated the trefoil knot as a possible source of d-dimensional UQC models through its subgroups of index d (corresponding to d-fold coverings of the T_1 three-manifold) (see [7] (Table 1)). More precisely, the link $L7n1$, corresponding to the congruence subgroup $\Gamma_0(2)$ of the modular group Γ, builds a relevant qutrit magic state for UQC whose MIC geometry is related to the Hesse configuration. The link $L6a3$, corresponding to the congruence subgroup $\Gamma_0(3)$ of Γ, builds a relevant two-qubit magic state whose MIC geometry is the generalized quadrangle of order two $GQ(2,2)$, as for the commutation of two-qubit Pauli operators. Then, the link identified by the software SnapPy as $L6n1$ (or sometimes $L8n3$), corresponding to the congruence subgroup $\Gamma(2)$ of Γ, defines a 6-ditMIC with a building block geometry looking like Borromean rings [6] (Figure 4). As shown in Section 2.2 below, none of the two links $L6n1$ and $L8n3$ are correctly associated with the subgroup $\Gamma(2)$ of Γ, but the link 6_3^3 (related to the Dynkin diagram of $\tilde{D}_4$) is. The possible confusion lies in the fact that all three links share the same link group $\pi_1(L)$. Finally, the link along the Dynkin diagram of D_4 (with the icosahedral symmetry of H_3 in the induced permutations) is associated with a 12-dimensional (two-qubit/qutrit) MIC corresponding to the congruence subgroup $10A^1$ of Γ [6] (Table 1).

1.2. Contents of the Work

As announced in the Abstract, we introduce a Seifert surface algorithm for converting the UQC models based on the aforementioned links into the appropriate braid representation permitted by Alexander's theorem [11]. These calculations are described in Section 2. A Seifert surface is an oriented surface whose boundary is a given link. Of course, it is not unique. In this paper, to generate a Seifert surface, one makes use of the braid representation of the link. Since it has a skein relation different from the one obeyed by anyons, this kind of topological quantum computation cannot be anyon-based. The skein relation in question is in terms of the Alexander polynomial instead of the Jones polynomial. In Section 3, taking into account the observation that some of our UQC models are related to affine Coxeter–Dynkin diagrams, we build a class of UQC models starting with affine Dynkin diagrams of type $\tilde{D}_4$, $\tilde{E}_6$, and $\tilde{E}_8$, which are singular fibers of minimal elliptic surfaces. Along the way, topological objects such as the three-torus, the Poincaré dodecahedral space [12], as well as the first amphicosm [13] are encountered. They are the precursors of the four-manifold topology that is currently under active scrutiny [14–16]. Its possible role in models of UQC is discussed in the Conclusion.

2. Seifert Surfaces and Braids from d-Fold Coverings of the Trefoil Knot Manifold (or of Hyperbolic Three-Manifolds)

Alexander's theorem states that every knot or link can be represented as a closed braid [11]. A Seifert surface F of a knot K or a link L is an oriented surface within the three-sphere S^3 whose boundary ∂F coincides with that knot or link. Given a basis $\{f_k\}$ for the first homology group $H_1(F;\mathbb{Z})$ of F, one defines a Seifert matrix V whose $(i,j)^{\text{th}}$ entry is the linking number of the component f_i and the positive push-off f_j^+ of the component f_j along a vector field normal to F. Then, an invariant of L is the (symmetrized) Alexander polynomial [11,15] (Section 2.7):

$$\Delta_L(t) = t^{-r/2}\det(V - tV^T), \tag{1}$$

with V^T the transpose of V and r the first Betti number of F. By definition, $\Delta_L(t^{-1}) = \Delta_L(t)$.

There exists a property of $\Delta_L(t)$ called a skein relation (the Jones polynomial used for defining anyons obeys a different skein relation than the Alexander polynomial [9,17], so that the rules for braiding are also different from those resulting from the Seifert surfaces). If L_+, L_0, and L_- are links in S^3, with projections differing from each other by a single crossing, as in Figure 1b, then:

$$\Delta_{L_+}(t) - \Delta_{L_-}(t) = (t^{1/2} - t^{-1/2})\Delta_{L_0}(t). \tag{2}$$

When L is a knot K, there is a connection of $\Delta_K(t)$ with a combinatorial invariant ν of the three-manifold S^3_K obtained from the zero-surgery along K in S^3 as follows:

$$\nu(S^3_K) = \frac{\Delta_K(t)}{(t^{1/2} - t^{-1/2})^2}. \tag{3}$$

The invariant $\nu(S^3_K)$ is called Milnor (or Reidemeister) torsion [18,19]. The invariant ν has the ability to distinguish closed manifolds, which are homotopy equivalent while being non homeomorphic.

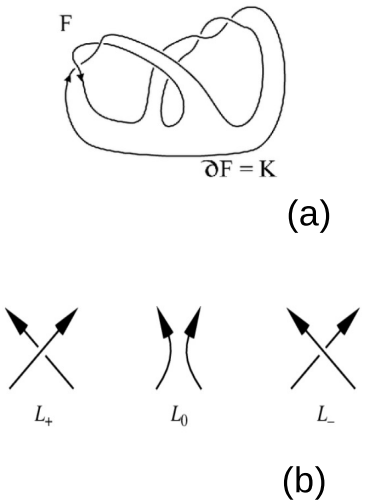

Figure 1. (**a**) The Seifert surface F for a trefoil knot K and (**b**) the types of crossings for the skein relation of a link L.

There exists a procedure for producing infinite families of homeomorphic, but non-diffeomorphic four-manifolds. It consists of applying a so-called Fintushel–Stern surgery along a torus T using some knot K. The so-obtained non-diffeomorphic four-manifolds may be distinguished thanks to the Seiberg–Witten invariant in which the Alexander polynomial $\Delta_K(e^{2T})$ appears as a factor [16] (Chapter 12).

The Seifert surface can be drawn from the braid representation. A good reference is [20] and a related website [21]. The software SeifertView provides a visualization of the Seifert surface [22]. In practice, to obtain the braid representation and the corresponding Alexander polynomial, we proceed as follows. In Figures 2–4 below, the braids are oriented from left to right and thus provide an orientation to the corresponding links. With the software SnapPy [23], one defines the link from its name (e.g., *M = Manifold* ("3_1") for the trefoil knot $K = T_1$) or from its PD representation available after drawing the link in the pink editor (e.g., *trefoil* = $[(6,4,1,3),(4,2,5,1),(2,6,3,5)]$, *L = Link(trefoil)* and *L.braid_word()* for obtaining the braid associated with T_1 as [-1,-1,-1], and *L.braid_matrix()* for obtaining the Seifert matrix V). Then, with Magma software [24], the Alexander polynomial follows (*det:= Determinant* $(u * V - v * Transpose(V))$*; det;* to obtain $u^2 - u * v + v^2$ or $t - 1 + t'$ after replacing u by $t^{1/2}$ and v by $t' = t^{1/2}$).

Results are summarized in Table 1.

Table 1. A few models of universal quantum computation (UQC) [7,25] translated into the language of braids and their Seifert surfaces. The source is a knot (such as the trefoil knot) or a link, and the target is a link L associated with a degree d covering of the L-manifold that defines an appropriate magic state for UQC and a corresponding minimal informationally-complete (MIC) measure. Cases $d = 3, 4, 5, ...$ correspond to the Hesse configuration, to the generalized quadrangle of order two $GQ(2,2)$ (also called a doily), to the Petersen graph. The notation for the braids is that of [20]. The notation t' means t^{-1}.

Source	Target	MIC	Braid Word	Alexander Polynomial
trefoil	L7n1	QTHesse	$(ab)^3b$	$t^{5/2} - t^{3/2} + t'^{(3/2)} - t'^{(5/2)}$
.	L6a3	2QBdoily	*ABCDCbaCdEdCBCDCeb*	$-3t^{1/2} + 3t'^{(1/2)}$
.	6_3^3	6-ditMIC	$(ab)^3$	$t^2 - t - t' + t^2$
.	D_4 Dynkin	2QB-QT MIC	*ABCCbaCCBCCb*	$-t^{3/2} + 3t^{1/2} + t'^{(3/2)} - 3t'^{(1/2)}$
fig. eight	L10n46	2QB doily	*abCbabbcBc*	$-t^{5/2} + 4t^{3/2} - 4t^{1/2} + \cdots$
.	L14n55217	7-dit MIC	*AbbcbcbDacBacdcb*	$-t^4 + 7t^3 - 11t^2 + 8t - 6 + \cdots$
Whitehead	L12n1741	QT Hesse	AbcDEFeDCBDacBdcdEdfCbdCddddeD	$-2t^3 + 6t^2 - 6t + 4 + \cdots$
.	L13n11257	5-dit MIC	AbCCbDaCBcDcDcbCD	$t^{9/2} - 6t^{7/2} + 15t^{5/2} - 21t^{3/2} + 21t^{1/2} + \cdots$
$6_3^2 = L6a1$	L12n2181	QT Hesse	ABcdEFceGbdFaedCBcdEdfcEgbdfedc	$4t^{5/2} - 12t^{3/2} + 16t^{1/2} + \cdots$
.	L14n63905	2QB doily	AbCddEdFedcBdaEdfCbceDccDcBC	$t^4 - 7t^3 + 22t^2 - 41t + 50 + \cdots$
L6a5	L14n63788	QT Hesse	ABCdEEEFEDcebdacEbEED ceDefedCeBdCEDe	$t^4 - 2t^3 + 2t - 2 + \cdots$

Before going further, let us recall the homomorphism between the conjugacy classes of subgroups of index d of a group G and the d-fold coverings of a manifold $\mathcal{M}$ whose fundamental group is $G = \pi_1(\mathcal{M})$ [26]. This relationship is not one-to-one (not an isomorphism) in the sense that a $\pi_1(\mathcal{M})$ may characterize distinct manifolds $\mathcal{M}$. A simple example is the number η_d of d-coverings of a manifold with characteristic $2g - 2 = 0$ (with g the genus) where η_d equals the sum of divisor function $\sigma(d)$ [27] (Section 3.4). Similarly, it is found in Section 2.2 that distinct links L =L6n1, L8n3, 6_3^3, and L_K define manifolds with a fundamental group of common cardinality sequence $\eta_d(L)$.

2.1. The Braids Built from the Trefoil Knot that Are Associated with the Qutrit Link L7n1 and the Two-Qubit Link L6a3

As announced in the Introduction, one refers to [7] (Table 1), which lists the topological properties of d-fold coverings $d = 1 \ldots 8$ of the trefoil knot manifold, as obtained from SnapPy, and also identifies the corresponding congruence subgroups of Γ previously investigated in [6]. From now on, one denotes $a, b, \ldots$ the generators of the fundamental group π_1, one uses the notation $A = a^{-1}, B = b^{-1}, \ldots$ for their inverses, and (.,.) means the group theoretical commutator of the entries. The link $L7n1$ corresponds to the congruence subgroup $\Gamma_0(2)$ of Γ. Its fundamental group $\pi_1 = \langle a, b | (a, B^2) \rangle$ builds a qutrit magic state for UQC of the type $(0, 1, \pm 1)$ and an MIC with the Hesse geometry [7] (Figure 1a). Figure 2a

is the drawing of $L7n1$. The braid representation $(ab)^3b$ is in Figure 2b, and the Seifert surface is in Figure 2c.

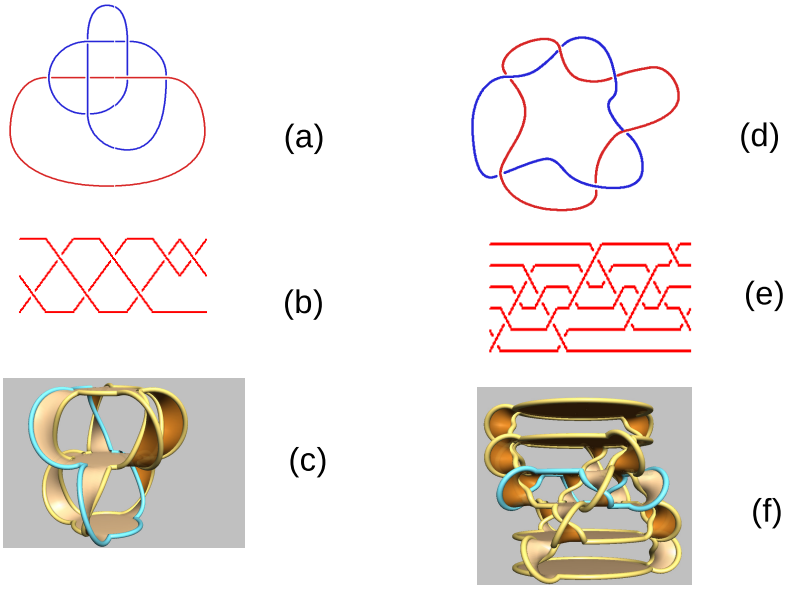

Figure 2. (**a**) The link $L7n1$ defining the qutrit MIC, (**b**) the braid representation, and (**c**) the corresponding Seifert surface. (**d**) The link $L6a3$ defining the two-qubit MIC, (**e**) the braid representation, and (**f**) the Seifert surface.

The link $L6a3$ corresponds to the congruence subgroup $\Gamma_0(3)$ of Γ. Its fundamental group $\pi_1 = \langle a, b | (a, b^3) \rangle$ builds a two-qubit magic state for UQC of the type $(0, 1, -\omega_6, \omega_6 - 1)$, $\omega_6 = \exp(\frac{2i\pi}{6})$, as well as an MIC with the geometry of the generalized quadrangle of order two $GQ(2, 2)$ (sometimes called a doily) [7] (Figure 1b). Figure 2d is the drawing of $L6a3$, Figure 2e the corresponding braid $ABCDCbaCdEdCBCDCeb$, and Figure 2f the Seifert surface.

The Alexander polynomials are given in Table 1.

2.2. The Braid Built from the Trefoil Knot that Is Associated with the 6-dit Link 6_3^3 and Related Braids with the Same Fundamental Group

There are eight conjugacy classes of subgroups of index six of the modular group Γ corresponding to eight six-fold coverings over the trefoil knot manifold. They are listed and identified in [7] (Table 1). We are first interested in the unique regular covering of degree six with homology group $\mathbb{Z} + \mathbb{Z} + \mathbb{Z}$ (with $\mathbb{Z}$ the group of integers) and three cusps corresponding to the congruence subgroup $\Gamma(2)$, which we denote $\mathcal{M}_6$,. The fundamental group is $\pi_1 = \langle a, b, c | (a, B), (b, C) \rangle$. The cardinality sequence of subgroups for the fundamental group of this particular covering is that of the link 6_3^3:

$$\eta_d(6_3^3) = [1, 7, 16, 60, 122,\ 794, 4212, 35276, 314949,\ \ldots] \tag{4}$$

It turns out that every degree six covering of the trefoil manifold leading to a 6-dit MIC (with a magic state of the type $(0, 1, \omega_6 - 1, 0, -\omega_6, 0)$, $\omega_6 = \exp(\frac{2i\pi}{6})$) shares the same fundamental group. For $\mathcal{M}_6$, SnapPy randomly provides several choices such as $L6n1$ or $L8n3$, which of course, share the same cardinality sequence as 6_3^3. In the Knot Atlas at "http://katlas.org/wiki/L6n1", one finds the sentence "$L6n1$ is 6_3^3 in Rolfsen's table of links". However, that seems to be a wrong statement.

Let us observe that by performing $(-2,1)$ surgery on all three cusps of $\mathcal{M}_6$ or of 6_3^3 and introducing the Dynkin diagram $\tilde{E}_6$ of affine E_6 (see Section 3 for details), one gets:

$$\eta_d[\mathcal{M}_6(-2,1)] = \eta_d[6_3^3(-2,1)] = \eta_d(\tilde{E}_6)$$
$$= [1,1,4,2,1,\ 6,3,2,10,1,\ 1,19,3,3,14,\ 3,1,36,3,2,\ \ldots],$$

while performing $(-2,1)$ surgery on cusps of $L6n1$ and introducing the Dynkin diagram of E_6, one gets:

$$\eta_d[L6n1(-2,1)] = \eta_d(E_6) = \eta_d(2T)$$
$$= [1,0,1,1,0,1,0,1,0,0,0,1,0,0,0,0,0,0,0,0,0,0,1,0,\ \ldots],$$

where $2T$ is the binary tetrahedral group.

We do not provide the result of performing $(-2,1)$ surgery on $L8n3$, which provides a still different result that we could not identify. We conclude that the correct identification of the manifold M should be 6_3^3, although we do not yet have a rigorous proof.

The link 6_3^3, the corresponding braid $(ab)^3$, and the Seifert surface are shown in Figure 3a–c. Switching the up/down positions of circles at two points (as shown in Figure 2c) provides the Kirby link L_K drawn in [28] (Figure 3) that we reproduce in Figure 3d (applying the surgeries as $L_K(4,1)(1,1)(2,1)$ to red, blue, and green circles, one gets the Brieskorn sphere $\Sigma(2,3,5)$, alias the Poincaré dodecahedral space). The corresponding braid word $aBabAb$ and its Seifert surface are in Figure 3e,f. It is notable that $(-2,1)$ surgery on K leads to the Dynkin diagram for A_3 of Weyl group S_4. Both links 6_3^3 and K have the same Alexander polynomial $t^2 - t - t' + t^2$.

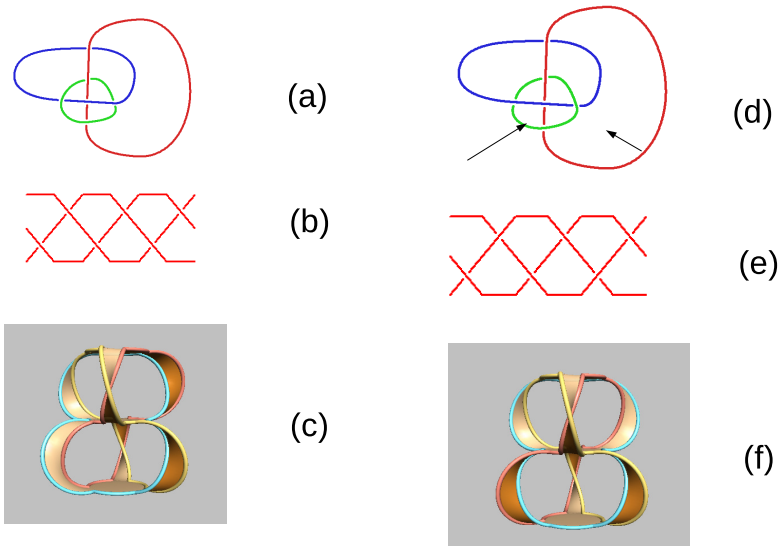

Figure 3. (**a**) The link 6_3^3 corresponding to the 6-dit MIC and the congruence subgroup $\Gamma(2)$ of Γ, (**b**) the braid representation, and (**c**) the Seifert surface. (**d**) The Kirby link L_K (see the arrows for the up/down changes), (**e**) the braid representation, and (**f**) the Seifert surface (observe the color changes).

The Six-Cover of the Trefoil Knot Manifold Corresponding to the Congruence Subgroup $3C^0$ of Γ

Let us conclude this subsection by another observation concerning the six-cover (that we denote M') of the trefoil knot manifold identified in [7] (Table 1) corresponding to the congruence subgroup $3C^0$. Again, the cardinality sequence of subgroups of $\pi_1(M')$ is that of 6_3^3, $L6n1$, $L8n3$, or L_K, but M' can be distinguished from the manifolds corresponding to these links since one gets under -2-surgery

$\eta_d[M'(-2,1)] = \eta_d[\tilde{D}_4]$, where $\tilde{D}_4$ is the Dynkin diagram of affine D_4 (as well as the smallest elliptic singular fiber of Kodaira's classification; see Figure 5a). Kodaira's classification may be found in [16] (p. 320) or [29] (Table 1).

2.3. The Braid Built from the Trefoil Knot that Is Associated with the Two-Qubit/Qutrit MIC with Icosahedral Symmetry of the Permutation Representation

In [6] (Table 1), the first author identified a two-qubit/qutrit MIC corresponding to the congruence subgroup $10A^1$ of the modular group Γ. The geometry of this MIC is that of the four-partite graph $K(3,3,3,3)$. More precisely, the subgroup of index 12corresponding to $10A^1$ is generated as $G = \langle a,b,c,d|(a,b),(a,c),(a,t)\rangle$, which corresponds to the fundamental group of a link along the Dynkin diagram of D_4. It builds a magic state for UQC of the type $(1,1,0,0,0,0,-\omega_6,-\omega_6,0,\omega_6-1,0,\omega_6-1)$. Under $(-2,1)$ surgery on all four components of the link attached to D_4, one recovers the quaternion group. The permutation representation that organizes the cosets of $10A^1$ in Γ is the icosahedral group $\mathbb{Z}_2 \times PSL(2,5)$, alias the Coxeter group of the Dynkin diagram H_3. The braid word and the corresponding Alexander polynomial are given in Table 1, and the Seifert surface is in Figure 4.

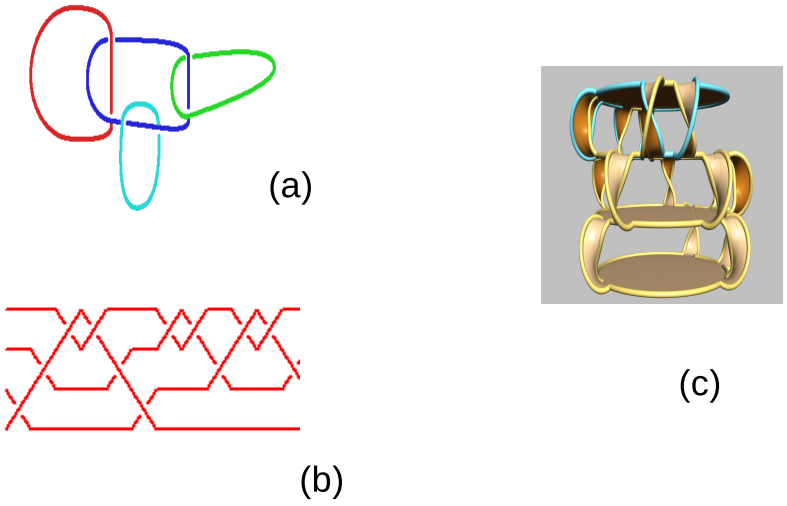

Figure 4. (**a**) The Dynkin diagram for the D_4 manifold attached to the 2QB-QT MIC, (**b**) the corresponding braid $ABCCbaCCBCCb$, and (**c**) the Seifert surface.

2.4. Braids from d-Fold Coverings of Hyperbolic Three-Manifolds

Models of UQC from MICs are also sometimes associated with links, as already recognized in [7,25]. Some of them are listed in Table 1 together as a corresponding braid word and Alexander polynomial.

2.4.1. The Hyperbolic Link $L10n46$ and Its Zero-Surgery

Let us focus on the figure-eight knot three-manifold that we call $\mathcal{M}_{K4a1}$. The low degree coverings over $\mathcal{M}_{K4a1}$ are three-manifolds that may be identified with SnapPy (see [7] (Table 2)). In particular, there are two coverings of degree four. One is cyclic with a single cusp and homology group $\mathbb{Z}/13 + \mathbb{Z}/15 + \mathbb{Z}$ and corresponds to the three-manifold otet08_{00007}. The second one is irregular with two cusps, has the homology group $\mathbb{Z} + \mathbb{Z}$, and corresponds to the complement of the link $L10n46$ (alias the hyperbolic three-manifold otet08_{00002}) (there is a mistake in [7] (Table 2). Some items have to be switched in the two degree four coverings over the figure-eight knot manifold.). The latter case defines a 2QB MIC and may be realized as a braid. The braid word is $abCbabbcBc$, and the Alexander polynomial is $-t^{5/2} + 4t^{3/2} - 4t^{1/2} + \cdots$.

Performing zero-surgery on both cusps of $L10n46$, one gets the same cardinality sequence, that from zero-surgery on the single cusp of figure-eight knot $K4a1$, as follows:

$$\eta_d[L10n46(0,1)] = \eta_d[K4a1(0,1)] = [1,1,1,\mathbf{2},2,\ \mathbf{5},1,2,\mathbf{2},4,\ \mathbf{3},17,1,1,2,\ \ldots].$$

The manifold defined by zero-surgery on the figure-eight knot is denoted Y in [30] where it is viewed as the boundary of a four-manifold with the rational homology of $S^1 \times D^3$ (a circle times a three-disk). It is found that any homology sphere obtained by integral surgery on Y bounds a rational homology ball.

The manifold Y is also investigated in [31] as a spontaneous surgery producing a manifold that is a fiber bundle over S^1 with the fiber a torus and an Anosov monodromy. The manifold has a "Sol"-type geometric structure in Thurston's classification of three-manifolds.

On our side, one finds that MICs result from irregular coverings of degrees 4, 6, 9 and 11 (this is emphasized with bold characters in the above sequence). The first case (leading to the 2QB MIC) has the homology $\mathbb{Z}$ and the same cardinality structure of subgroups as Y itself; the permutation group organizing the cosets is the permutation representation of the congruence subgroup $\Gamma_0(3)$ of the modular group Γ. In the second case (leading to a two-valued 6-dit MIC), the homology is $\mathbb{Z}/4 + \mathbb{Z}/4 + \mathbb{Z}$, and the permutation group organizing the cosets is the permutation representation of the congruence subgroup $3C^0$ of Γ. The next case corresponds to a two-valued 2QT MIC (QT means qutrit).

Finally, from (3), one mentions that with zero-surgery on the figure-eight knot $K = K4a1$, one gets the Reidemeister torsion of K, and it is given through the Alexander polynomial $\Delta(K) = -t + 3 - t'$.

2.4.2. Further Results

As shown in Table 1, there also exists a seven-cover over $\mathcal{M}_{K4a1}$ that is associated to a 7-dit MIC and the link $L14n55217$ (alias the three-manifold $\mathcal{M}'$ =otet14_{00002}).

Other models happen to be more complicated. We do not describe them in more detail.

3. Quantum Computing from Affine Dynkin Diagrams

In the previous section, we found that some MICs for UQC (our approach of universal quantum computing with complete quantum information) relate to Coxeter–Dynkin diagrams: $\tilde{E_6}$ and $\tilde{D_4}$ for the 6-dit MIC and D_4 for the two-qubit/qutrit MIC. This is an unexpected observation that we would like to complete by another one: the possibility of defining UQC from the singular fiber $II^* = \tilde{E_8}$ of Kodaira's classification of minimal elliptic surfaces (see Figure 5c). This classification is used in the understanding of some aspects of the four-manifold topology as shown in [16] (p. 320); see also [32] for a different perspective.

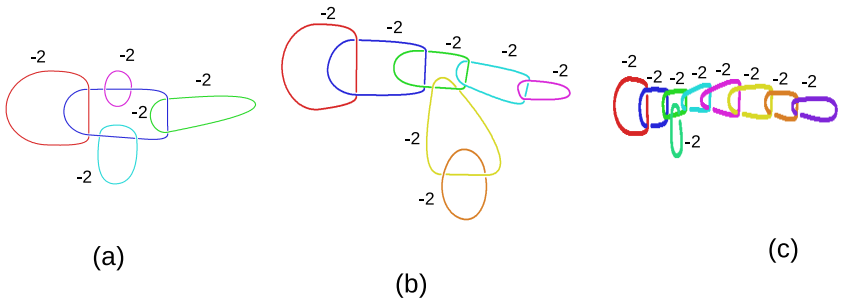

Figure 5. A few singular fibers in Kodaira's classification of minimal elliptic surfaces. (**a**) Fiber I_0^* (alias $\tilde{D_4}$), (**b**) fiber IV^* (alias $\tilde{E}_6$), and (**c**) fiber II^* (alias $\tilde{E}_8$).

Taking $\pi_1(\tilde{E}_8)$ as the fundamental group of affine E_8, the subgroup structure of $\pi_1(\tilde{E}_8)$ has the following cardinality list:

$$\eta_d(\tilde{E}_8) = [1, 1, \mathbf{2}, \mathbf{2}, 1,\ \mathbf{5}, \mathbf{3}, 2, 4, 1,\ 1, 12, \mathbf{3}, 3, \mathbf{4},\ \ldots] \tag{5}$$

where the bold characters mean that at least one of the subgroups leads to an MIC, as in [7]. It is worthwhile to observe that the boundary of the manifold associated to $\tilde{E}_8$ is the Seifert fibered toroidal manifold [33], denoted Σ' in [7] (Table 5). It may also be obtained by zero-surgery on the trefoil knot T_1.

For the sequence above, the coverings are:

$$[\tilde{E}_8, \tilde{E}_6, \{\tilde{D}_4, \tilde{E}_8\}, \{\tilde{E}_6, \tilde{E}_8\}, \tilde{E}_8,\ \{BR_0, \tilde{D}_4, \tilde{E}_6\}, \{\tilde{E}_8\}, \{\tilde{E}_6\}, \{\tilde{D}_4, \tilde{E}_8\}, \tilde{E}_6, \tilde{E}_8, \{BR_0, \tilde{D}_4, \tilde{E}_6, \tilde{E}_8\}, \{\tilde{E}_8\}, \{\tilde{E}_6\}, \{\tilde{D}_4, \tilde{E}_8\}, \cdots]$$

One observes that the subgroups/coverings are fundamental groups for $\tilde{E}_8$ $\tilde{E}_6$, $\tilde{D}_4$, or BR_0, where BR_0 is the manifold obtained by zero-surgery on all circles of Borromean rings. The cardinality sequence of subgroups of BR_0 is:

$$\eta_d(BR_0) = [1, 7, 13, 35, 31,\ 91, 57, 155, 130, 217,\ \cdots] \tag{6}$$

which is recognized as A001001 in Sloane's encyclopedia of integer sequences with the title "Number of sublattices of index d in generic three-dimensional lattice".

As already given in Section 1, the subgroup structure of $\pi_1(\tilde{E}_6)$ has the following cardinality list:

$$\eta_d(\tilde{E}_6) = [1, 1, 4, \mathbf{2}, 1,\ 6, 3, 2, 10, 1,\ \ldots]. \tag{7}$$

For this sequence, the coverings are:

$$[\tilde{E}_6, \tilde{E}_6, \{BR_0, \tilde{E}_6\}, \tilde{E}_6, \tilde{E}_6,\ \{BR_0, \tilde{E}_6\}, \{\tilde{E}_6\}, \{\tilde{E}_6\}, \{BR_0, \tilde{E}_6\}, \tilde{E}_6 \cdots].$$

The subgroup structure for $\tilde{D}_4$ is:

$$\eta_d(\tilde{D}_4) = [1, 7, 5, 23, 7,\ 39, 9, 65, 18, 61,\ \cdots] \tag{8}$$

which corresponds to A263825 in Sloane's encyclopedia of integer sequences with the title "Total number $c_{\pi_1(B_1)}(n)$ of n-coverings over the first amphicosm B_1' [13].

To be exhaustive, let us mention that $\tilde{E}_7$ is III^* Kodaira's singular fiber. Following [29] (Table 1), it can be obtained by $(-2, 1)$-surgery on the link $L4a1$ (in [29] (Table 1), II^* is $3_1(0, 1)$, III^* is $L4a1(-2, 1)$, and $IV^* = 6_3^3(-2, 1)$, as one expects). Observe that $L4a1$ has the same fundamental group as $L7n1$ (see Section 2.1) and $\eta_d[L4a1(-2, 1)] = \eta_d(\tilde{E}_7) = [1, 3, 1, 7, 3,\ 5, 1, 16, 2, 11, \cdots]$.

$\tilde{E}_7$ has coverings of type BR_0, $\tilde{D}_4$, and $\tilde{E}_7$, which we do not detail here.

Reidemeister Torsion of the Manifold Σ'

As a final note for this section, according to (3), the "twisted" Reidemeister torsion ν_t of the three-manifold obtained from zero-surgery along a knot K in S^3 is the Alexander polynomial of K. The zero-surgery on the trefoil knot $T_1 = 3_1$ defines the Seifert fibered toroidal manifold Σ' introduced in Section 3, and one gets $\nu_t(S^3_{T_1}) = \nu_t(\Sigma') = t - 1 + t'$.

Let $BR = L6a4$ be the Borromean rings and the manifold BR_0 as above (obtained by zero-surgery on all circles of BR) and BR_1 be the manifold obtained by zero-surgery on two circles of BR. The cardinality sequence $\eta_d(BR_0)$ is as in (6), and $\eta_d(BR_1)$ is found as in (4). In principle, one can compute the Reidemeister torsion for BR_0 and BR_1 [19] (Section 2.4). This is left open in this paper.

4. Conclusions

In the first part of this paper, it has been found that some coverings of the trefoil knot, or of other knots or links, that are used for informationally-complete universal quantum computing are three-manifolds originating from a link within the three-sphere. From the braid representation of such links, we defined Seifert surfaces and computed the Alexander polynomials. We pointed out that some coverings of the trefoil knot (of index 6 and index 12, respectively) connect to the symmetry of Dynkin diagrams (affine E_6 and D_4). In the second part, it has been found that the singular fiber $\tilde{E}_8$ may be used to generate UQC and that its coverings are the singular fibers $\tilde{E}_6$ and $\tilde{D}_4$ (alias the first amphicosm), as well as the manifold BR_0 obtained by zero-surgery on all circles of Borromean rings. Generalizing the analysis to coverings of $\tilde{D}_4$ and BR_0, one finds that the three-torus enters the game [12].

While a Jones polynomial controls an anyon braid, the Alexander polynomial controls the braid-induced Seifert surface. Further work is in progress to connect our work to the theory of four-manifolds and the Seiberg–Witten invariant [14,16]. For instance, braided surfaces wrapped around singularities within four-manifolds support quasiparticles [34]. Another motivation for three- and four-dimensional topological quantum computing concerns the foundations of quantum gravity [35]. Topological invariants are important in topological quantum field theory and its application to quantization in general relativity, through loop quantum gravity [36,37]. In this context, starting from a pure topological action, it is possible to address the quantization of general relativity with its diffeomorphism invariance. Topological invariants play an essential role in defining and computing quantum amplitudes in these models, and it is tentative to associate them with topological quantum computing.

Author Contributions: All authors contributed substantially to the research. Conceptualization: M.P. and K.I.; methodology, M.P.; software, M.P. and R.A.; validation, R.A. and M.M.A.; formal analysis, M.P. and M.M.A.; investigation, M.P., R.A., and M.A.; resources, R.A and K.I.; data curation, M.P.; writing, original draft preparation, M.P.; writing, review and editing, M.P. and M.M.A.; supervision, K.I.; project administration, M.P. and K.I.; funding acquisition, K.I.

Funding: The research was funded by Quantum Gravity Research, Los Angeles, CA.

Conflicts of Interest: The authors declare no conflict of interest.

References

1. Bravyi, S.; Kitaev, A. Universal quantum computation with ideal Clifford gates and noisy ancillas. *Phys. Rev.* **2005**, *A71*, 022316. [CrossRef]
2. Veitch, V.; Mousavian, S.A.; Gottesman, D.; Emerson, J. The resource theory of stabilizer quantum computation. *New J. Phys.* **2014**, *16*, 013009. [CrossRef]
3. Seddon, J.R.; Campbell, E. Quantifying magic for multi-qubit operations. *arXiv* **2019**, arXiv:1901.03322.
4. Planat, M.; Haq, R.U. The magic of universal quantum computing with permutations. *Adv. Math. Phys.* **2017**, *217*, 5287862. [CrossRef]
5. Planat, M.; Gedik, Z. Magic informationally complete POVMs with permutations. *R. Soc. Open Sci.* **2017**, *4*, 170387. [CrossRef]
6. Planat, M. The Poincaré half-plane for informationally complete POVMs. *Entropy* **2018**, *20*, 16. [CrossRef]
7. Planat, M.; Aschheim, R.; Amaral, M.M.; Irwin, K. Universal quantum computing and three-manifolds, Universal quantum computing and three-manifolds. *Symmetry* **2018**, *10*, 773. [CrossRef]
8. Freedman, M.; Kitaev, A.; Larsen, M.; Wang, Z. Topological quantum computation. *Bull. Am. Math. Soc.* **2003**, *40*, 31. [CrossRef]
9. Kauffman, L.H.; Lomonacco, S.J. Braiding, Majorana fermions, Fibonacci particles and topological quantum computing. *Quant. Inf. Proc.* **2018**, *17*, 201. [CrossRef]
10. Nayak, C. Non-Abelian Anyons and Topological Quantum Computation. *Rev. Mod. Phys.* **2008**, *80*, 1083. [CrossRef]

11. Adams, C.C. *The Knot Book, An Elementary Introduction to the Mathematical Theory of Knots*; W. H. Freeman and Co.: New York, NY, USA, 1994.
12. Weeks, J.R. *The Shape of Space*, 2nd ed.; Chapman & Hall: Boca Raton, FL, USA, 2001; 408p.
13. Chelnokov, G.; Deryagina, M.; Meldnykh, A. On the coverings of Euclidean manifolds $\mathcal{B}_1$ and $\mathcal{B}_2$. *Commun. Algebra* **2017**, *45*, 1558. [CrossRef]
14. Gompf, R.E.; Stipsicz, A.I. *four-Manifolds and Kirby Calculus*; Graduate Studies in Mathematics; American Mathematical Society: Providence, RI, USA, 1999; p.129.
15. Akbulut, S. *four-Manifolds*; Oxford Graduate Texts in Mathematics 25; Oxford University Press: Oxford, UK, 2016.
16. Scorpian, A. *The Wild World of four-Manifolds*; American Mathematical Society: Providence, RI, USA, 2005.
17. Kauffman, L.H. State models and the Jones polynomial. *Topology* **1987**, *26*, 395–407. [CrossRef]
18. Milnor, J. A duality theorem for Reidemeister torsion. *Ann. Math. Sec. Ser.* **1962**, *76*, 137–147. [CrossRef]
19. Nicolaescu, L.I. Notes on the Reidemeister Torsion. Available online: http://www.nd.edu/~lnicolae/ (accessed on 1 February 2019).
20. Van Wijk, J.J.; Cohen, A.M. Visualization of Seifert surfaces. *IEEE Trans. Vis. Comput. Graph.* **2006**, *12*, 485–496. [CrossRef]
21. Collins, J. Seifert Matrix Computations. Available online: www.maths.ed.ac.uk/~v1ranick/julia/index.htm (accessed on 1 November 2018).
22. van Wijk, J.J.; Cohen, A.M. SeifertView a Program to Visualize Seifert Surfaces in 3D. Available online: www.win.tue.nl/~vanwijk/seifertview (accessed on 1 November 2018).
23. Culler, M.; Dunfield, N.M.; Goerner, M.; Weeks, J.R. SnapPy, a Computer Program for Studying the Geometry and Topology of three-Manifolds. Available online: http://snappy.computop.org (accessed on 1 November 2018).
24. Bosma, W.; Cannon, J.J.; Fieker, C.; Steel, A. (Eds.) *Handbook of Magma Functions*; University of Sydney: Sydney, Australia, 2017; 5914p.
25. Planat, M.; Aschheim, R.; Amaral, M.M.; Irwin, K. Quantum computing with Bianchi groups. *arXiv* **2018**, arXiv:1808.06831.
26. Mednykh, A.D. A new method for counting coverings over manifold with finitely generated fundamental group. *Dokl. Math.* **2006**, *74*, 498–502. [CrossRef]
27. Liskovets, V.A.; Mednykh, A.D. On the number of connected and disconnected coverings over a manifold. *Ars. Math. Contemp.* **2009**, *2*, 181. [CrossRef]
28. Kirby, R.C.; Scharlemann, M.G. Eight faces of the Poincaré homology three-sphere. In *Geometric Topology*; Academic Press: New York, NY, USA, 1979; pp 113–146.
29. Kirby, R.C.; Melvin, P. The E_8-manifold, singular fibers and handlebody decompositions. *Geom. Topol. Publ.* **1998**, *2*, 233–258.
30. Akbulut, S.; Larson, K. Brieskorn spheres bounding rational balls. *Proc. Am. Math. Soc.* **2018**, *146*, 1817–1824. [CrossRef]
31. Hilden, H.; Lozano, M.T.; Montesinos-Amilibia, J.M. On a remarkable polyhedron geometrizing the figure eight cone manifolds. *J. Math. Sci. Univ. Tokyo* **1995**, *2* 501–561.
32. Aschheim, R.; Irwin, K. Constructing numbers in quantum gravity: Infinions. In Proceedings of the Group32 Conference, Prague, Czech Republic, 9–13 July 2018.
33. Wu, Y.-Q. Seifert fibered surgery on Montesinos knots. *arXiv* **2012**, arXiv:1207.0154.
34. Atiyah, M.; Marcolli, M. Anyons in geometric models of matter. *J. High Energ. Phys.* **2017**, *76*. [CrossRef]
35. Asselmeyer-Maluga, T.; Król, J. How to obtain a cosmological constant from small exotic $\mathbb{R}^4$. *Phys. Dark Univ.* **2018**, *19* 66–77. [CrossRef]
36. Rovelli, C.; Vidotto, F. *Covariant Loop Quantum Gravity*, 1st ed.; Cambridge University Press: Cambridge, UK, 2014.
37. Amaral, M.; Aschheim, R.; Irwin, K. Quantum gravity at the fifth root of unity. *arXiv* **2019**, arXiv:1903.10851.